

# Effects of Ti Addition on Microstructure and Magnetic Properties of B-rich $\text{Nd}_{9.4}\text{Fe}_{79.6-x}\text{Ti}_x\text{B}_{11}$ Nanocrystalline Alloys

Li Shun, Bai Shuxin, Zhang Hong, Chen Ke, Xiao Jiayu

National University of Defense Technology, Changsha 410073, China

**Abstract:** The effects of Ti addition on the microstructure and magnetic properties of  $\text{Nd}_{9.4}\text{Fe}_{79.6-x}\text{Ti}_x\text{B}_{11}$  ( $x=0, 1, 2, 4, 6$ ) nanocrystalline alloys were investigated. The results show that Ti addition suppresses the formation of unfavorable soft  $\text{Nd}_2\text{Fe}_{23}\text{B}_3$  and  $\text{Fe}_3\text{B}$  phases, and promotes the formation of  $\text{Nd}_2\text{Fe}_{14}\text{B}$  phases. When the Ti content reaches a certain amount, Ti may precipitate as  $\text{TiB}_2$  from the alloys.  $\text{TiB}_2$  may serve as inoculants and promotes uniform nucleation, and thus increases the exchange coupling between the hard and soft phases. As a result, excellent magnetic properties of  $B_r=0.87$  T,  $H_{cj}=931$  kA/m and  $(BH)_{\max}=115.4$  kJ/m<sup>3</sup> are achieved in  $\text{Nd}_{9.4}\text{Fe}_{75.6}\text{Ti}_4\text{B}_{11}$  alloy ribbons.

**Key words:** nanocomposite magnets; microstructure; permanent magnet; demagnetization curve

Nanocomposite permanent magnets composed of hard magnetic phases with high anisotropic field and soft magnetic phases with large saturation magnetization have attracted much attention for permanent applications. In the magnets, when the hard and soft phase are intimately mixed on the scale of the Bloch wall thickness, which for hard phases is of 10–30 nm<sup>[1]</sup>, the mixtures no longer appear to act as like two independent phases, and the hysteresis loop looks similar to that of a conventional single phase permanent magnet. In the study of anisotropic nanocomposite magnets with an ideal microstructure, Skomski and Coey<sup>[2]</sup> pointed out that a potential maximum energy products up to 1 MJ/m<sup>3</sup> has been achieved, which is about two times of that of the sintered Nd-Fe-B magnets with the highest maximum energy products. Nowadays, nanocomposite permanent magnets have been produced for commercial use, but their maximum energy products are still far lower than the theoretic value which is probably due to the incomplete exchange coupling between the hard and soft magnetic phases. In the nanocomposite magnets, the addition of small concentrations of refractory elements such as Zr, Nb or Ti has been reported which is useful for controlling the

growth of the soft and hard phase, resulting in refining the structure, and increasing the exchange coupling interaction between the soft and hard phases<sup>[3–6]</sup>. However, the above mentioned literatures are most concentrated on the microstructure and magnetic properties of low B content  $\text{Nd}_2\text{Fe}_{14}\text{B}/\alpha\text{-Fe}$  nanocrystalline alloys, and there is a little understanding on the underlying mechanism of refractory element addition to improve the magnetic properties of B-rich nanocrystalline alloys. So in this paper, the effects of Ti addition on the microstructure and magnetic properties of B-rich Nd-Fe-B nanocrystalline alloys were investigated and discussed.

## 1 Experimental

Starting materials were high purity Nd, Fe, and Ti metals with purity greater than 99.5%, and Fe-B alloys with B content of 20.22%. Alloy ingots with nominal compositions of  $\text{Nd}_{9.4}\text{Fe}_{79.6-x}\text{Ti}_x\text{B}_{11}$  ( $x=0, 1, 2, 4, 6$ ) were arc-melted in a high purity Ar atmosphere for at least four times to insure homogeneity. Ribbons were prepared from small pieces of crushed ingots by the single-roller melt-spinning technique at various

Received date: February 21, 2008

Foundation item: Science and Technology Ministry of Changsha

Biography: Li Shun, Candidate for Ph. D., Department of Material Engineering and Applied Chemistry, National University of Defense Technology, Changsha 410073, P. R. China, Tel: 0086-731-4576147, E-mail: linudt@163.com

Copyright © 2009, Northwest Institute for Nonferrous Metal Research. Published by Elsevier BV. All rights reserved.

surface speed in a high purity argon atmosphere. Selected ribbons were sealed in a quartz tube in argon and then annealed at 600–700 °C for 4 min to generate magnetic properties. Phases existing in the melt-spun ribbons were identified with powder X-ray diffraction (XRD) using a Cu-K $\alpha$  radiation. Magnetic properties of the ribbons were measured with a vibrating sample magnetometer. The microstructures of the ribbons were investigated with a transmission electron microscopy (TEM). A Netzsch-STA449C differential scanning calorimeter (DSC) was used for thermal analysis of as-spun ribbons at a heating rate of 15 °C/min. Thermal magnetic analyzer (TMA) was used to determine the Curie temperature of magnetic phases with an externally magnetic field of 0.2 T.

## 2 Results and Discussion

Fig.1 shows the X-ray diffraction (XRD) patterns of Nd<sub>9.4</sub>Fe<sub>79.6-x</sub>Ti<sub>x</sub>B<sub>11</sub> (x=0, 1, 2, 4, 6) alloy ribbons which were subjected to an optimal crystallization treatment. From the XRD patterns it can be seen that with increasing of Ti, the intensity of  $\alpha$ -Fe peak exhibits a progressive decrease, indicating that Ti suppresses the formation and growth of the soft  $\alpha$ -Fe phases. The half peak breadth of  $\alpha$ -Fe and Nd<sub>2</sub>Fe<sub>14</sub>B becomes large with the increase of Ti addition, reflecting the effect of Ti as a grain size controller according to the Scherrer formula<sup>[7]</sup>.

Because of overlapping of diffraction peaks between Nd<sub>2</sub>Fe<sub>14</sub>B phase and Nd<sub>2</sub>Fe<sub>23</sub>B<sub>3</sub> or other B-rich phases, Thermal Magnetic Analyzer (TMA) was used in order to clearly indicate the phases of the alloy ribbons after crystallization. Fig.2 shows the TMA curves of Nd<sub>9.4</sub>Fe<sub>79.6</sub>B<sub>11</sub> and Nd<sub>9.4</sub>Fe<sub>75.6</sub>Ti<sub>4</sub>B<sub>11</sub> ribbons after optimal crystallization treatment. As can be seen, there are four magnetic phases, i.e. magnetically hard Nd<sub>2</sub>Fe<sub>14</sub>B, magnetically soft Nd<sub>2</sub>Fe<sub>23</sub>B<sub>3</sub>, Fe<sub>3</sub>B and  $\alpha$ -Fe, which present in the Nd<sub>9.4</sub>Fe<sub>79.6</sub>B<sub>11</sub> alloy ribbons. With the addition of Ti, there are only two magnetic phases, i.e. magnetically hard Nd<sub>2</sub>Fe<sub>14</sub>B, and magnetically soft  $\alpha$ -Fe appear in the Nd<sub>9.4</sub>Fe<sub>75.6</sub>Ti<sub>4</sub>B<sub>11</sub> alloy ribbons, which suggests that Ti suppresses the formation of soft Nd<sub>2</sub>Fe<sub>23</sub>B<sub>3</sub> and Fe<sub>3</sub>B phases, consequently resulting in the formation of Nd<sub>2</sub>Fe<sub>14</sub>B/ $\alpha$ -Fe mixture.

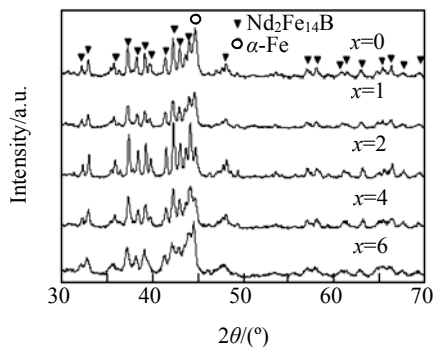


Fig.1 XRD patterns of Nd<sub>9.4</sub>Fe<sub>79.6-x</sub>Ti<sub>x</sub>B<sub>11</sub> (x=0, 1, 2, 4, and 6) ribbons subject to their optimal crystallization treatment

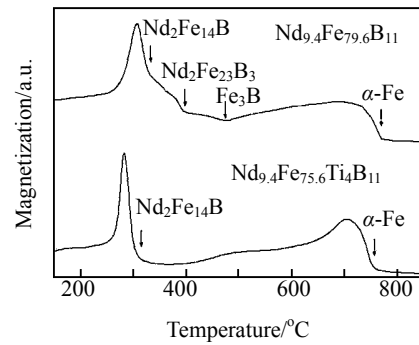


Fig.2 TMA curves of alloy ribbons following their optimal crystallization treatment

Magnetic properties of Nd<sub>9.4</sub>Fe<sub>79.6-x</sub>Ti<sub>x</sub>B<sub>11</sub> (x=0, 1, 2, 4, 6) melt-spun ribbons which were subjected to an optimal crystallization treatment are presented in Fig.3. Clearly,  $H_{cj}$  increases progressively as the Ti content increases, from 479 kA/m for x=0 to 965 kA/m for x=6.  $B_r$  increases from 0.83 T for x=0 to 0.92 T for x=2 at first, and then decreases monotonously.  $(BH)_{max}$  increases significantly upon the adding of Ti, from 73.2 kJ/m<sup>3</sup> up to 122.5 kJ/m<sup>3</sup> when x=2, with a slight drop for x=4 and 6. Large  $H_{cj}$  values are in the range from 668 kA/m for x=2 to 963 kA/m for x=6, suggesting the smaller volume fraction of soft magnetic phases. The magnetic properties of Nd<sub>9.4</sub>Fe<sub>79.6-x</sub>Ti<sub>x</sub>B<sub>11</sub> alloys are obviously improved with the addition of Ti. Excellent magnetic properties of  $B_r=0.87$  T,  $H_{cj}=931$  kA/m and  $(BH)_{max}=115.4$  kJ/m<sup>3</sup> can be obtained in Nd<sub>9.4</sub>Fe<sub>75.6</sub>Ti<sub>4</sub>B<sub>11</sub> alloy ribbons.

Fig.4 presents the DSC curves of amorphous Nd<sub>9.4</sub>Fe<sub>79.6</sub>B<sub>11</sub> and Nd<sub>9.4</sub>Fe<sub>75.6</sub>Ti<sub>4</sub>B<sub>11</sub> melt-spun ribbons. For Nd<sub>9.4</sub>Fe<sub>79.6</sub>B<sub>11</sub> ribbons, there is a large exothermic peak showing two peak values, which are located at about 603.4 °C and 647.9 °C respectively. This phenomenon may be related to the formation of  $\alpha$ -Fe, Nd<sub>2</sub>Fe<sub>14</sub>B, Nd<sub>2</sub>Fe<sub>23</sub>B<sub>3</sub> and Fe<sub>3</sub>B phases according to the above XRD and TMA analysis. For Nd<sub>9.4</sub>Fe<sub>75.6</sub>Ti<sub>4</sub>B<sub>11</sub> ribbons with Ti addition, there are two exothermic peaks, which are located at about 647.6 °C and 702.0 °C respectively. This

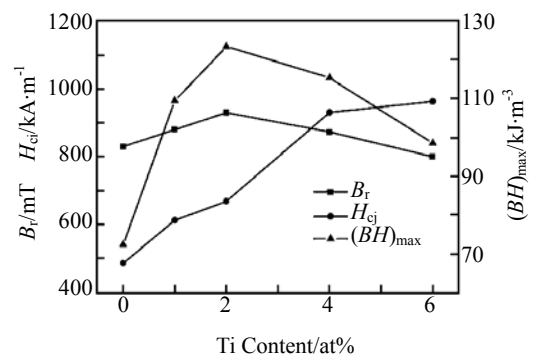


Fig.3 Magnetic properties of Nd<sub>9.4</sub>Fe<sub>79.6-x</sub>Ti<sub>x</sub>B<sub>11</sub> (x=0, 1, 2, 4, 6) alloy ribbons subjected to an optimal crystallization treatment

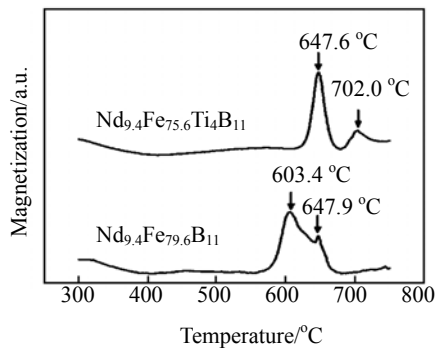


Fig.4 DSC curves of Nd<sub>9.4</sub>Fe<sub>79.6</sub>B<sub>11</sub> and Nd<sub>9.4</sub>Fe<sub>75.6</sub>Ti<sub>4</sub>B<sub>11</sub> alloys ribbons

behavior is corresponding to the formation of  $\alpha$ -Fe and Nd<sub>2</sub>Fe<sub>14</sub>B. The addition of Ti suppresses the formation of Nd<sub>2</sub>Fe<sub>23</sub>B<sub>3</sub> phase and Fe<sub>3</sub>B phase and increases the crystallization temperature. According to the theory of nucleation<sup>[8]</sup>, the nucleation rate follows an Arrhenius law. The crystallization at higher temperature means that more grains will be nucleated per unit time, which is of avail for attaining a fine and uniform microstructure.

Transmission electron micrographs for two selected nanocomposite alloys, Nd<sub>9.4</sub>Fe<sub>79.6</sub>B<sub>11</sub> and Nd<sub>9.4</sub>Fe<sub>75.6</sub>Ti<sub>4</sub>B<sub>11</sub>, after optimal crystallization treatment, are displayed in Fig.5a and Fig.5b, respectively. For the Ti-free sample, Fig.5a shows an inhomogeneous microstructure comprised of small grains and much large grains (about 100 nm), and their average grain size is about 50–60 nm, which would reduce the strength of exchange coupling effect between the hard and soft grains, leading to incomplete exchange coupling and thus, to inferior magnetic properties for the composite structure. Furthermore, the large soft grains would become the nuclei of the reverse magnetic domain and consequently initiate a cascade-type demagnetization process of the alloy.

For the alloy with 4 at% Ti addition (Fig.5b), the microstructure with a homogeneous grain size distribution and average grain size of about 30–40 nm can be achieved. A fine and uniform microstructure is essential to induce a high ex-

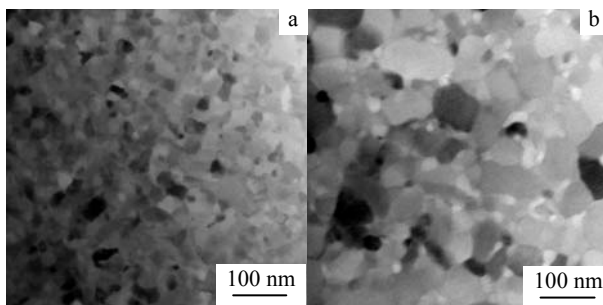


Fig.5 TEM micrographs of the optimally annealed alloy ribbons: (a) Nd<sub>9.4</sub>Fe<sub>79.6</sub>B<sub>11</sub> and (b) Nd<sub>9.4</sub>Fe<sub>75.6</sub>Ti<sub>4</sub>B<sub>11</sub>

change coupling between Nd<sub>2</sub>Fe<sub>14</sub>B phases and  $\alpha$ -Fe phases, which leads to the enhanced  $H_{cj}$  and  $(BH)_{max}$ .

D. J. Branagan and R. W. McCallum<sup>[9]</sup> showed that Ti has significant non-equilibrium solubility for Nd<sub>2</sub>Fe<sub>14</sub>B phase, but after homogenization, the equilibrium solubility of Ti for Nd<sub>2</sub>Fe<sub>14</sub>B phase is reduced to about 0.47 wt%. In Nd<sub>9.4</sub>Fe<sub>75.6</sub>Ti<sub>4</sub>B<sub>11</sub> alloy, the content of Ti is about 3.14 wt%, which is much larger than the equilibrium solubility of Ti. Therefore, stable Ti-phases may precipitate from Nd<sub>9.4</sub>Fe<sub>75.6</sub>Ti<sub>4</sub>B<sub>11</sub> alloy ribbons after crystallization. In Ti-doped Nd-Fe-B alloy, stable binary phases, such as TiFe, TiFe<sub>2</sub>, TiB, Ti<sub>3</sub>B<sub>4</sub>, and TiB<sub>2</sub>, may form. Among these stable binary phases, TiB<sub>2</sub> has the largest enthalpy of about –108 kJ/mol. So, when Ti is added to Nd<sub>9.4</sub>Fe<sub>79.6</sub>B<sub>11</sub> alloy, it might be expected that TiB<sub>2</sub> will form owing to its extremely high free energy of formation. However, TiB<sub>2</sub> was not detected by X-ray diffraction for the small amount of it. But Y. Kitano<sup>[10]</sup> confirmed the existence of TiB<sub>2</sub> in Nd-Fe-B magnets with Ti additions.

Stable TiB<sub>2</sub> phases do not dissolve and are not easy to grow at high temperatures which may serve as inoculants and promote uniform nucleation. When Ti content is high, large amount of TiB<sub>2</sub> may form. Although the grain size controlling effect is stronger, a low remanence together with a high coercivity will be achieved in Nd<sub>9.4</sub>Fe<sub>73.6</sub>Ti<sub>6</sub>B<sub>11</sub> alloy ribbon owing to the reduced volume fraction of magnetically hard Nd<sub>2</sub>Fe<sub>14</sub>B phases.

### 3 Conclusion

Obvious enhancements of magnetic properties can be obtained in Ti substituted B-rich Nd<sub>9.4</sub>Fe<sub>79.6-x</sub>Ti<sub>x</sub>B<sub>11</sub> ( $x=0, 1, 2, 4, 6$ ) nanocrystalline alloy ribbons. The enhancement reason is attributed to two factors. First, Ti suppresses the formation of unfavorable soft Nd<sub>2</sub>Fe<sub>23</sub>B<sub>3</sub> and Fe<sub>3</sub>B phases and results in Nd<sub>2</sub>Fe<sub>14</sub>B/ $\alpha$ -Fe mixture. Second, stable TiB<sub>2</sub> phases appear in Ti-doped Nd-Fe-B alloys which serve as inoculants and promote uniform nucleation, and thus increase the exchange coupling interaction between the soft and hard phases; an increase of coercivity is achieved. As a result, excellent magnetic properties of  $B_r=0.87$  T,  $H_{cj}=931$  kA/m and  $(BH)_{max}=115.4$  kJ/m<sup>3</sup> are achieved in Nd<sub>9.4</sub>Fe<sub>75.6</sub>Ti<sub>4</sub>B<sub>11</sub> alloy ribbons.

### References

- Kneller E F, Hawig R. *IEEE Trans on Magn*[J], 1991, 27: 3588
- Skomski R, Coey J M D. *Phys Rev B* [J], 1993, 48: 15812
- Jianua A, Valeanua M, Lazar D P et al. *J Magn Magn Mater*[J], 2004, 272–276: 1493
- Chen Z M, Wu Y Q, Kramer M J et al. *J Magn Magn Mater*[J], 2004, 268: 105
- Chang W C, Wang S H, Chang S J et al. *IEEE Trans Magn*[J], 1999, 35: 3265

- 6 Wang Wei(王伟), Ni Jiansen(倪建森), Zhou Xiyong(周细应) et al. *Rare Metal Materials and Engineering*(稀有金属材料与工程)[J], 2005, 34: 1051
- 7 Gui Lifeng(桂立丰), Tang Rujun(唐汝钧). *Handbook of Materials Testing for Mechanical Engineering*(机械工程材料测试手册)[M]. Liaoning: Liaoning Science and Technology Press, 1999
- 8 Wang Yihe(王一禾), Yang Yingshan(杨膺善). *Metallic Glasses* (非晶态合金) [M]. Beijing: Metallurgy Industry Press, 1990
- 9 Branagan D J, McCallum R W. *J Alloys Compd*[J], 1995, 230: 67
- 10 Kitano Y, Shomomura J. *J Appl Phys*[J], 1991, 69: 6055

## Ti 对高 B 含量纳米复合 $\text{Nd}_{9.4}\text{Fe}_{79.6-x}\text{Ti}_x\text{B}_{11}$ 永磁合金显微结构和磁性能的影响

李 顺, 白书欣, 张 虹, 陈 柯, 肖加余  
(国防科技大学, 湖南 长沙 410073)

**摘 要:** 研究了 Ti 添加对  $\text{Nd}_{9.4}\text{Fe}_{79.6-x}\text{Ti}_x\text{B}_{11}$  ( $x=0, 1, 2, 4, 6$ ) 合金显微结构和磁性能的影响。结果表明, 添加 Ti 能抑制  $\text{Nd}_{9.4}\text{Fe}_{79.6-x}\text{Ti}_x\text{B}_{11}$  合金中  $\text{Nd}_2\text{Fe}_{23}\text{B}_3$  和  $\text{Fe}_3\text{B}$  相的形成及  $\alpha\text{-Fe}$  相的析出和长大, 促进  $\text{Nd}_2\text{Fe}_{14}\text{B}$  相的形成。当 Ti 添加到一定量时, Ti 能以  $\text{TiB}_2$  质点的形式从合金中析出,  $\text{TiB}_2$  质点能够抑制晶粒的长大, 改善合金的显微结构。综合性能比较佳的  $\text{Nd}_{9.4}\text{Fe}_{75.6}\text{Ti}_4\text{B}_{11}$  合金薄带最佳退火工艺下剩磁  $B_r$  为 0.87 T, 矫顽力  $H_{cj}$  达到 931 kA/m, 磁能积  $(BH)_{\max}$  为 115.4 kJ/m<sup>3</sup>。

**关键词:** 纳米复合磁体; 显微结构; 永磁体; 退磁曲线

---

**作者简介:** 李 顺, 男, 1981 年生, 博士生, 国防科技大学材料工程与应用化学系(一院五系)501 教研室, 湖南 长沙 410073, 电话: 0731-4576147, E-mail: linudt@163.com